

## Spiral wave drift in an electric field and scroll wave instabilities

Hervé Henry

Center for Theoretical Biological Physics, University of California San Diego, 9500 Gilman Drive, La Jolla, California 92093

(Received 27 October 2003; revised manuscript received 18 May 2004; published 11 August 2004)

Here, I present the numerical computation of speed and direction of the drift of a spiral wave in an excitable medium in the presence of an electric field. The drift speed presents a strong variation close to the parameter value where the drift-speed component along the field direction from parallel becomes antiparallel. Using a simple phenomenological model and results from a numerical linear stability analysis of scroll waves, I show that this behavior can be attributed to a resonance of the meander modes with the translation modes of the spiral wave. Extending this phenomenological model to scroll waves also clarifies the link between the drift and long wavelength instabilities of scroll waves.

DOI: 10.1103/PhysRevE.70.026204

PACS number(s): 05.45.Pq, 87.19.Hh

Spiral waves can be observed in a variety of excitable systems such as Belousov-Zhabotinsky gels [1], colonies of the *dictyostelium* amoebae [2], and slices of cardiac tissue [3]. In the latter example, spiral waves of electrical activity have been shown to be the source of ventricular tachycardia and some of their instabilities are believed to be involved in the transition from tachycardia to fibrillation, a deadly arrhythmia (for a review see [4]). This, with the intrinsic interest of those structures, has led to an important research effort in order to understand the dynamic and instabilities of spiral waves and of their three-dimensional, analogous, scroll waves.

In the presence of an external electric field, in the Belousov-Zhabotinsky (BZ) reaction, the center of rotation of spiral waves drift with a speed that presents components both parallel and perpendicular to the applied field [5]. The parallel component of the drift speed was always found to be in the direction of the applied field. A numerical study [6] showed that depending on the parameter regime, the drift direction of the spiral could be either parallel or antiparallel to the field. The drift of a spiral wave has been linked [7,8] to the curvature instability of scroll waves [9,10] that leads scroll waves to bend, and can finally result in a fibrillation-like disordered activity of the medium. It was also linked to the three-dimensional meander of scroll waves [11], which is the three-dimensional analog of the meander instability [12,13] characterized by a periodic modulation of the radius of rotation of the spiral wave. This phenomenon has been studied from a theoretical point of view [6,8,14,15]. However, most analytical studies are restricted to the large core [8] or the small core limit [16] and cannot examine the observed change in drift direction.

In this paper, I present results of numerical computations that show an unexpected behavior of the drift speed at the drift direction change. The drift speed varies strongly in the vicinity of the transition. Using a reduced model of spiral wave in the presence of a small electric field, I show that this phenomenon can be attributed to a resonance between meander and translation modes of spiral waves. Finally, using the analogy between the effect of an electric field and the effects of a slight curvature of a scroll wave, I extend this model to scroll waves. This extension sheds some light on the link between the drift of a spiral wave in an electric field and long

wavelength instabilities of scroll waves, and results obtained from this model are in good agreement with the results of the numerical linear stability analysis of scroll waves [7].

I begin with describing the results of a numerical study of the spiral dynamics in the presence of an electric field using the Barkley model of an excitable medium (contrary to BZ systems,  $u$  is the only diffusive variable),

$$\partial_t u = \frac{1}{\epsilon} f(u, v) + \Delta u + E \partial_x u, \quad (1)$$

$$\partial_t v = g(u, v), \quad (2)$$

where  $f(u, v) = u(1-u)[u-(v+b)/a]$ ,  $g(u, v) = u-v$ , and  $E$  is the electric field, directed along the  $x$  axis. A homogeneous system modeled by these equations presents a single stable equilibrium point  $u=v=0$  and a small perturbation of this equilibrium point can lead to a large excursion in phase space before return to equilibrium. The diffusive coupling in Eq. (1) allows the propagation of solitary waves in one dimension. In two dimensions, in the absence of an electric field ( $E=0$ ), a rich variety of wave propagation regime is observed depending on the values of the parameters [17]. I will focus here on steadily rotating spirals and present results obtained along a line of equation  $b=0.13$  in the parameter space of [17] (along this line no meandering spiral is observed).

In the presence of the electric field ( $E \neq 0$ ), the spiral tip drifts with a constant velocity (see Fig. 1) that depends on the parameter values and on the electric field strength. The drift velocity has components perpendicular ( $v_{\perp}$ ) and parallel ( $v_{\parallel}$ ) to the field. These velocities vary linearly with the field in the small  $E$  limit. This allows us to define the drift coefficient  $\alpha_{\perp} = v_{\perp}/E$  and  $\alpha_{\parallel} = v_{\parallel}/E$  [24] in a weak field.

Numerical results (see Fig. 2) show that close to the transition from antiparallel to parallel drift, the value of  $E$  for which the linear regime is reached is much smaller than for the small  $a$  and large  $a$  region. In addition, close to this transition, the dependence of the drift coefficients  $\alpha_{\parallel} + i\alpha_{\perp}$  in  $a$  is strongly nonmonotonous. When increasing  $a$ , there is a strong enhancement of the parallel drift coefficient followed by a relatively sharp transition from parallel to antiparallel

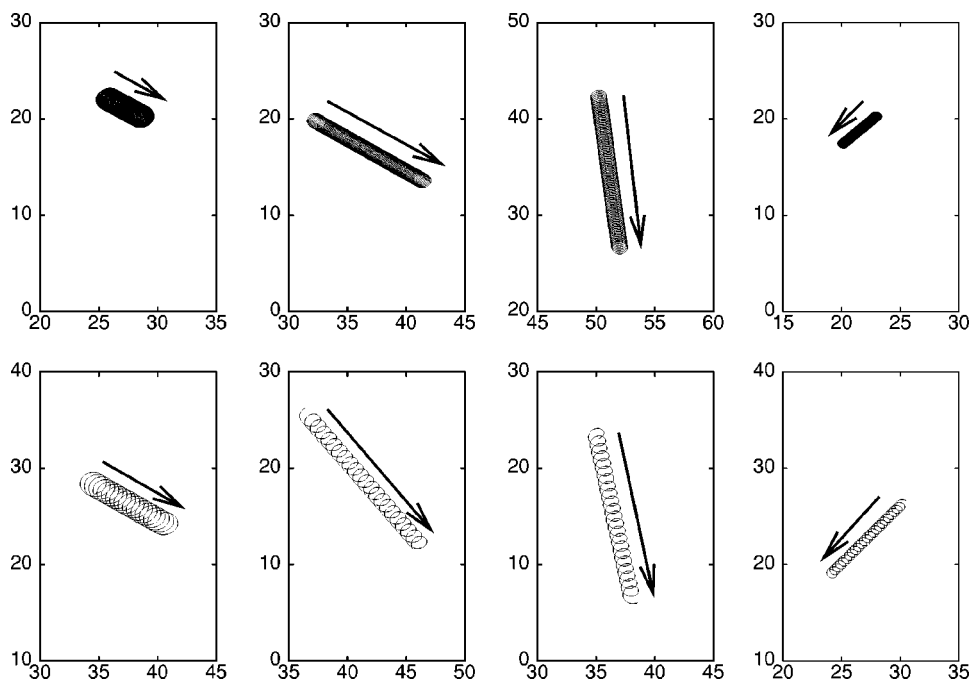


FIG. 1. Tip trajectories in the presence of an electric field for  $a$  equal (left to right) to 0.85, 0.91, 0.93, and 0.99 for  $E=0.03$  (top) and  $E=0.003$  (bottom). (Other parameter values are  $b=0.13$  and  $\epsilon=0.02$ .) The trajectories were recorded for 100 time units (tu) (top) and 400 tu (bottom) and are represented in boxes of same spatial extension. The arrows show the drift direction. For parameter values  $a=0.85$  and 0.99, the drift velocity behaves almost linearly with the strength of the field (this was checked by performing two simulations, see also Fig. 2 (one should note that this is enough to check whether the linear regime is reached, since an additional point is  $v=0, E=0$ ) while in the cases  $a=0.91$  and 0.93 the behavior is still strongly nonlinear.

drift, and finally, the drift coefficients decrease rapidly. The behavior of the perpendicular drift coefficient is characterized by a strong enhancement close to the value of  $a$  where the transition occurs. These results differ strongly from the results presented in [6], where the drift speeds were computed using the same parameter values and an electric field of amplitude  $E=0.3$ : a monotonic variation of the drift speeds with the parameter values, which is also observed here when using high values of  $E$  for which (see Fig. 2, solid line) the drift amplitude is no longer linear with the field amplitude.

I now present an ordinary differential equations (ODE) model of spiral wave drift in an electric field that explains the strong enhancement of drift coefficients by the resonance of damped meander modes and translation modes. The ODE model is a modification of models [17,18] that reproduces the main feature of the spiral wave dynamics and has been modified in order to take into account the effects of a small electric field [19]:

$$\dot{r} = e^{i\phi}(R_0\omega_t - z) + \beta E, \tag{3}$$

$$\dot{z} = [\mu - i\omega_m - (1 + i\alpha)|z|^2]z + \gamma E e^{-i\phi}, \tag{4}$$

$$\dot{\phi} = \omega_t, \tag{5}$$

where  $r$  is the position of the tip in the complex plane  $[(x, y)$  in the real plane correspond to  $(\text{Re}, \text{Im})$  in the complex plane],  $z$  is a complex variable describing the meander in the frame rotating with the spiral,  $\mu + i\omega_m$  is the eigenvalue as-

sociated with the meander mode, and  $E$  is the amplitude of the field directed along the real axis in the imaginary plane. In the absence of an electric field ( $E=0$ ), for  $\mu < 0$ , the steady state is obtained for  $z=0$  and corresponds to the stationary rotating spiral  $r=R_0 \exp(i\omega_t t)$  at frequency  $\omega_t$ . For  $\mu > 0$ , the  $z=0$  solution of Eq. (4) is no longer stable and the  $z$  variable undergoes a Hopf bifurcation that leads to the modulation of the radius of curvature of the tip with frequency  $-\omega_m$  characteristic of meandering spirals [one should note that for  $\omega_t = \omega_m$ , the meander instability ( $\mu > 0$ ) leads to the drift of the rotating spiral with constant velocity [17] for  $E=0$ ].

I now give some rationale for the terms introduced in Eqs. (3)–(5). In Eq. (3), the effect of the field can be either independent of the relative orientation of the spiral and the field (the  $\beta E$  term) or depend on it. Nonetheless, the latter case leads to a precessing term that, when integrated over one spiral rotation, vanishes at dominant order. Hence, I have chosen to add only the former term and to disregard the latter, which would have no effect at leading order. The  $\gamma E \times \exp(-i\phi)$  term in Eq. (4) has to take into account that the field is constant in the laboratory frame, while Eq. (4) is expressed in the frame rotating with the spiral, that is the laboratory frame rotated of  $\phi$ . Therefore, it is necessary to add the  $\exp(-i\phi)$  factor, which expresses the fact that the meander mode is affected by the field in a way that depends on the relative orientations of the spiral and of the electrical field (in the frame rotating with the spiral the field is rotating with a pulsation, which is  $-\dot{\phi}$ ). No extra term has been added to Eq. (5) (also expressed in the frame rotating with the

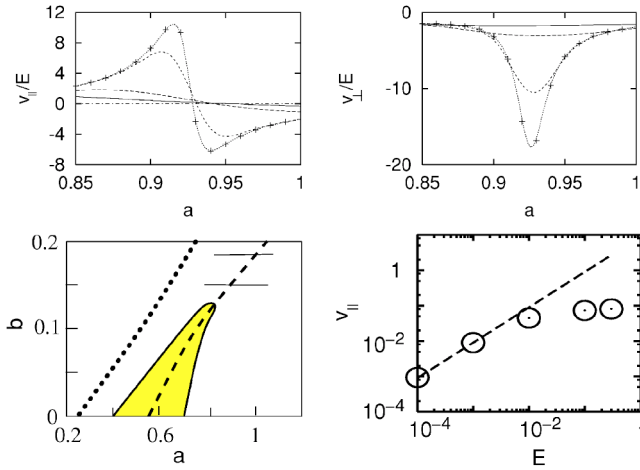


FIG. 2. Parameter values are  $\epsilon=0.02$  and  $b=0.13$ . Top left:  $v_{\parallel}/E$  for the following values of the applied external field: 0.3 (solid), 0.1 (long dashed), 0.01 (short dashed), 0.001 (dotted), 0.0001 (+), the dashed-dotted line is the line of the equation  $v_{\parallel}/E=0$ . Top right:  $v_{\perp}/E$  for the same values of the external field,  $E$ . Note that for both larger and smaller values of  $a$  (not shown here)  $v_{\parallel}/E$  and  $v_{\perp}/E$  are independent of  $E$  for the  $E$  range explored here. Note that the curves for  $E=0.0001$  and  $E=0.001$  are indistinguishable, indicating that for those values, the drift speed is linear in  $E$ . Hence the dotted curves also represent  $\alpha_{\perp}$  and  $\alpha_{\parallel}$ . One should note the very different shape of the two dotted curves. Similar results (with a not so strong drift enhancement) were observed for higher values of  $b$  and stronger damping of meander modes ( $b=0.18$ ). Bottom left: schematic of the phase diagram in Barkley's parameter space. In the region that is left of the dotted line, no spiral waves are observed. On the right-hand side of this line, rotating and meandering spiral waves (gray region) are observed. The dashed line corresponds roughly to  $\omega_m=\omega_t$  and the horizontal solid lines correspond to the values of  $b$  (0.13 and 0.18) for which systematic simulations were performed. Bottom right:  $v_{\parallel}$  as a function of  $\log_{10}E$  for  $a=0.92$  and  $b=0.13$ .  $E$  is varying from 0.0001 to 0.3 and the dashed line is of the equation  $v_{\parallel}=9.3v$ .

spiral), since at dominant order the addition of a term proportional to  $E \exp(-i\phi)$  would only lead to another constant drift term in Eq. (3) similar to the  $\beta E$  term.

I focus here on the case where steadily rotating spirals are stable (i.e.,  $\mu < 0$  and  $\omega_m$  is the frequency of the meander mode that can be computed by linear stability analysis [20] of steady spirals) and describe the effects of a small field in this situation. At the leading order in  $E$  and  $z$ , Eq. (4) has for solution  $z = A \exp(-i\omega_t t)$  with  $A = \gamma E / [-\mu + i(-\omega_t + \omega_m)]$ . Using this expression in Eq. (3) leads to a spiral tip drifting with constant velocity:

$$\frac{v_d}{E} = \beta + \frac{\gamma[\mu - i(\omega_t - \omega_m)]}{\mu^2 + (\omega_t - \omega_m)^2}. \quad (6)$$

This expression qualitatively describes the behavior of the spiral drift coefficients in the presence of an electric field as a function of  $a$ , presented in Fig. 2, if the two following conditions are met. First, close to the point where the transition from antiparallel to parallel drift occurs the meander frequency,  $\omega_m$  becomes equal to the spiral frequency  $\omega_t$  and

$\mu$  is small (*weakly damped meander regime*). Second, the real part of  $\gamma$  is much smaller than its imaginary part in this region. Else, the expression of Eq. (6) cannot qualitatively reproduce the behavior observed in Fig. 2. One can check this statement by looking at the value of the drift coefficient in the case where  $\gamma = i\gamma_i$  is imaginary. In this case, the expression of the drift speed is

$$\frac{v_d}{E} = \beta + \frac{\gamma_i(\omega_t - \omega_m)}{\mu^2 + (\omega_t - \omega_m)^2} + i \frac{\gamma_i \mu}{\mu^2 + (\omega_t - \omega_m)^2}, \quad (7)$$

which well reproduces the behavior presented in Fig. 2 when  $\mu$  is small.

It is also interesting to note that the drift coefficient, as expressed in Eq. (6) diverges if  $\mu=0$  and  $\omega_m=\omega_t$ , that is, at the codimension two point of the Barkley phase space [17] (noted  $P$  here). This seems unphysical since in the absence of an electric field, one can see a perfectly stable spiral. Nonetheless, as shown in [17], for  $\omega_m=\omega_t$  and  $\mu > 0$  the meandering spiral tip trajectory is the one of a steadily drifting spiral with a constant finite speed even if  $E=0$  (this situation corresponds to the case of an infinite drift coefficient). Hence it is not surprising that the drift coefficient should diverge when approaching  $P$  in the stable spiral region.

The following part of this paper will show that these requirements are met. In addition, the link between the drift of a spiral wave and three-dimensional instabilities of scroll waves will be discussed. One can determine the values of  $\omega_t$  and  $\omega_m$  using the linear stability analysis of steady spiral previously described in [20] and extended to scroll waves in [7]. As seen in Fig. 3,  $\omega_t$  and  $\omega_m$  become equal for  $a \approx 0.925$  (i.e., close to the transition from antiparallel to parallel drift). In addition, for this value of  $a$ , the damping of meander mode is relatively weak. Finally, taking  $\gamma=0.4i$  and  $\beta=-0.36-1.3i$ , the behavior of the drift coefficients is well approximated by the expression of Eq. (6) in the vicinity of the transition.

Since the effects of a small electric field on a spiral are analogous to the effects of the slight curvature of a scroll wave, it is of interest to consider the three-dimensional extension of this model. In the following part of the paper, I will describe the results obtained using this simple model. The results presented here confirm that the low  $k_z$  curvature of the translation mode [7] is equal to the drift coefficients. They will also show that, contrary to what was hypothesized in [11], the drift coefficients are not equal to the opposite of the low  $k_z$  curvature of meander modes.

First, consider a slightly curved spiral filament. The evolution equations of  $u$  and  $v$  are the three-dimensional analog of Eqs. (1) and (2) in the case  $E=0$ . They can be rewritten using the coordinates  $s, X, Y$ , where  $s$  is the curvilinear abscissa along the spiral filament [21],  $X$  and  $Y$  are the Cartesian coordinates in the plane perpendicular to the filament (the  $X$  axis being oriented along the normal to the filament). Using this coordinate system and assuming a slight curvature of the filament, Eq. (2) is unchanged and Eq. (1) reads

$$\partial_t u = \frac{1}{\epsilon} f(u, v) + \Delta_{XY} u - \frac{1}{\rho - X} \partial_X u, \quad (8)$$

where  $\rho$  is the radius of curvature of the filament and  $\Delta_{XY}$  is the two-dimensional Laplacian operator in the  $XY$  plane. The

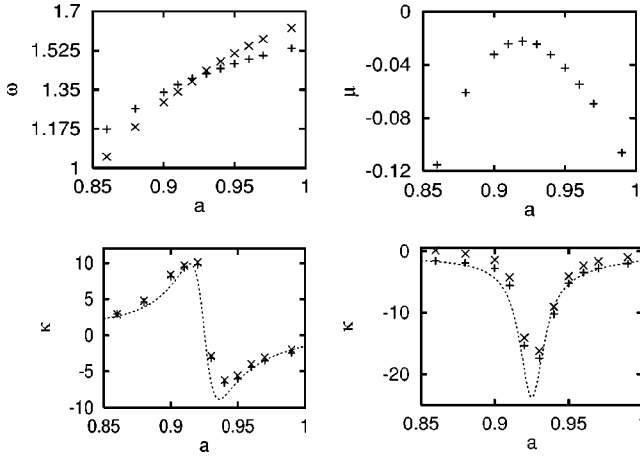


FIG. 3. Top left: computed frequencies of the meander mode ( $\times$ ) and of the translation mode (+) as a function of the control parameter  $a$  ( $\epsilon=0.02$  and  $b=0.13$ ).  $\omega_m$  and  $\omega_t$  are equal for  $a \approx 0.925$ . Top right: growth rate of the meander mode as a function of  $a$  (other parameters unchanged). The maximal value of  $\mu$  is reached for  $a \approx 0.920$ . Bottom left: curvatures of the real part of the translation branches (+) and opposite of the curvature of the real part of the meander branches ( $\times$ ) at  $k_z=0$ . Bottom right: Computed curvatures of the imaginary part of the translation branches and opposite of the curvature of the imaginary part of the meander branches at  $k_z=0$ . For  $a=0.92$  and  $0.93$ , the computed values of the curvatures present an uncertainty of order 1 due to the hybridization of meander and translation modes. The dashed lines in bottom figures show the fit obtained using Eq. (10) for the translation modes and a second-order polynomial fit of  $\gamma(a)$  and  $\beta(a)$ . The fit for the meander modes is not shown here.

$-[1/(\rho-X)]\partial_X u$  term, at leading order in  $X/\rho$  is equal to  $1/\rho$ . Hence in the new frame, close to the filament, Eq. (1) is affected by the curvature of the filament in the same way it is affected by an electric field  $E=-1/\rho$ .

Therefore, the three-dimensional extension of the Barkley-Sandstede model for slightly curved filaments is given by Eqs. (3)–(5) where  $E$  is replaced by  $-r''$  and where  $r''$  denotes the second-order derivative of  $r$  along the axis of the filament. For slightly curved filaments,  $r''$  is equal to the opposite of its curvature. A linear stability analysis of the tridimensional ODE model around the steady scroll wave [ $z=0, r_0(z, t)=\exp(i\omega_t t)$ ] in the frame rotating with the spiral, i.e., using a perturbation of the form  $r=r_0(z, t)+r_1 e^{i\phi} e^{\sigma t + ik_z z}$  and  $z=z_1 e^{\sigma t + ik_z z}$ , leads to the following eigenvalue problem:

$$\sigma \begin{pmatrix} r_1 \\ z_1 \end{pmatrix} = \begin{pmatrix} -i\omega_t + \beta k_z^2 & -1 \\ +\gamma k_z^2 & \mu - i\omega_m \end{pmatrix} \begin{pmatrix} r_1 \\ z_1 \end{pmatrix}, \quad (9)$$

whose eigenvalues are at leading order in  $k_z$ :

$$\sigma_t = -i\omega_t + \left[ \beta + \frac{\gamma}{\mu + i(\omega_t - \omega_m)} \right] k_z^2, \quad (10)$$

$$\sigma_m = \mu - i\omega_m - \left[ \frac{\gamma}{\mu + i(\omega_t - \omega_m)} \right] k_z^2. \quad (11)$$

These equations show that the curvature of the translation branch is equal to the opposite of the curvature of the mean-

der mode shifted of  $\beta$ . It is also equal to the drift speed [see Eq. (6)]. Hence, contrary to what was proposed by Aranson *et al.* [11], the curvature of the meander mode is not equal to the drift coefficients. There is a shift (that can be relatively small when the parameter values are close to the line where  $\omega_m = \omega_t$ ) as shown in Fig. 3. This might come from the fact that the parameter  $\beta$  was omitted in Ref. [11].

In addition, since the numerical linear stability analysis of scroll waves allows us to determine  $\sigma_t$ ,  $\sigma_m$ ,  $\mu$ ,  $\omega_t$ , and  $\omega_m$  for small values of  $k_z$ , one can extract from Eqs. (10) and (11) the expressions of the coefficients  $\beta$  and  $\gamma$ :

$$\beta = -(\kappa_m + \kappa_t), \quad (12)$$

$$\gamma = \kappa_m [\mu + i(\omega_t - \omega_m)], \quad (13)$$

$$\kappa_m = -(u_m \bullet \tilde{u}_m) / [(u_m \bullet \tilde{u}_m) + (v_m \bullet \tilde{v}_m)], \quad (14)$$

$$\kappa_t = -(u_t \bullet \tilde{u}_t) / [(u_t \bullet \tilde{u}_t) + (v_t \bullet \tilde{v}_t)], \quad (15)$$

where  $\kappa_m$  and  $\kappa_t$  the respective curvatures of meander and translation branches at  $k_z=0$  and can be expressed as functions of  $(u_m, v_m)$ ,  $(u_t, v_t)$  and the meander and translation modes,  $(\tilde{u}_m, \tilde{v}_m)$  are  $(\tilde{u}_t, \tilde{v}_t)$  are the corresponding adjoint modes that can be computed [22] and  $(\bullet)$  denotes the usual scalar product in the frame rotating with the spiral.

This method in the vicinity of  $\omega_m = \omega_t$  results in great variations in the values of  $\gamma$  since it is very sensitive to possible inaccuracies. However, for values of  $a$  away from the transition, one can compute both  $\beta(a)$  and  $\gamma(a)$  with a good accuracy. They appear then to be smooth functions of  $a$  that can be easily fitted by a second order in  $a$  polynomial. For  $a$  close to the transition from parallel to antiparallel drift, the polynomial fits of  $\beta(a)$  and  $\gamma(a)$  take values close to the ones used previously to fit the drift speed and using the polynomial fit in Eqs. (10) and (11) one reproduces with a good accuracy the results of the long wavelength linear stability analysis of scroll waves (see Fig. 3). One should also note that Eq. (13), together with the results of the numerical three-dimensional linear stability analysis of scroll waves, give some rationale for  $\gamma$  being an imaginary number close to the transition from antiparallel to parallel drift. Indeed, close to the transition,  $\kappa_m$  is mainly directed along the imaginary axis in the complex plane and  $\omega_m \approx \omega_t$ , those two results lead to  $\gamma$  being directed almost along the imaginary axis.

To conclude, using smoothly varying coefficients  $\beta$  and  $\gamma$ , this model quantitatively reproduces the results obtained numerically when considering both the drift of a spiral wave in the presence of an external field and the long wavelength instabilities of scroll waves (meander and curvature). The reduced model brings some clarification on the mechanism of the drift of a spiral wave in the presence of an electric field, showing that the change in the sign of drift velocity parallel to the electric field can be attributed to a resonance between meander and translation modes and that this resonance leads to a strong increase in the drift coefficients. One should also note that despite that the results presented here are formally valid for  $\mu \ll 1$ , the resonance described here influences the drift speed as a function of parameters for a



wider parameter regime and its effects can be observed rather far away from the Barkley's codimension two point [see Fig. 2(a) (inset)] as long as meander modes are not too damped. I also hope those results can be checked experimentally in a BZ system where meandering of spiral waves has been well characterized [23].

I wish to thank Vincent Hakim and Blas Echebarria for very fruitful discussions. I am also grateful to Wouter-Jan Rappel and Vincent Hakim for useful comments on early versions of this manuscript. This work was supported in part by the NFS-sponsored Center for Theoretical Biological Physics (Grant No. 0225630).

- 
- [1] A. Winfree, *Science* **175**, 634 (1972).  
 [2] I. Aranson, H. Levine, and L. Tsimring, *Phys. Rev. Lett.* **76**, 1170 (1996).  
 [3] A. T. Winfree, *When Time Breaks Down* (Princeton University Press, Princeton, NJ, 1987).  
 [4] F. Fenton, E. Cherry, H. Hastings, and S. Evans, *Chaos* **12**, 852 (2002).  
 [5] O. Steinbock, J. Schütze, and S. C. Müller, *Phys. Rev. Lett.* **68**, 248 (1992).  
 [6] V. Krinsky, E. Hamm, and V. Voignier, *Phys. Rev. Lett.* **76**, 3854 (1996).  
 [7] H. Henry and V. Hakim, *Phys. Rev. Lett.* **85**, 5328 (2000).  
 [8] V. Hakim and A. Karma, *Phys. Rev. E* **60**, 5073 (1999).  
 [9] V. N. Biktashev, A. V. Holden, and H. Zhang, *Philos. Trans. R. Soc. London, Ser. A* **347**, 611 (1994).  
 [10] S. Alonso, F. Sagues, and A. Mikhailov, *Science* **299**, 1722 (2003).  
 [11] I. Aranson and I. Mitkov, *Phys. Rev. E* **58**, 4556 (1998).  
 [12] A. Karma, *Phys. Rev. Lett.* **65**, 2824 (1990).  
 [13] D. Barkley, M. Kness, and L. Tuckerman, *Phys. Rev. A* **42**, 2489 (1990).  
 [14] H. Zhang, B. Hu, G. Hu, and J. Xiao, *J. Chem. Phys.* **119**, 4468 (2003).  
 [15] M. Wellner, A. Pertsov, and J. Jalife, *Phys. Rev. E* **59**, 5192 (1999).  
 [16] I. Mitkov, I. Aranson, and D. Kessler, *Phys. Rev. E* **52**, 5974 (1995).  
 [17] D. Barkley, *Phys. Rev. Lett.* **72**, 164 (1994).  
 [18] B. Sandstede and A. Scheel, *Phys. Rev. Lett.* **86**, 171 (2001).  
 [19] The modified model was built during a private conversation with B. Echebarria and V. Hakim.  
 [20] D. Barkley, *Phys. Rev. Lett.* **68**, 2090 (1991).  
 [21] J. P. Keener, *Physica D* **31**, 269 (1988).  
 [22] H. Henry and V. Hakim, *Phys. Rev. E* **65**, 046235 (2002).  
 [23] L. Ouyang, V. Petrov, and H. Swinney, *Phys. Rev. Lett.* **77**, 2105 (1996).  
 [24] To avoid ambiguity, the direction of  $v_{\perp}$  is defined as the drift velocity in the direction of  $\mathbf{E} \times \boldsymbol{\omega}$ , where  $\boldsymbol{\omega}$  is the frequency of the spiral and  $\mathbf{E}=(E,0)$ .